SECED 2023 Conference
Earthquake Engineering & Dynamics for a Sustainable Future
14-15 September 2023, Cambridge, UK

SUPERELASTIC FRICTION DAMPERS FOR RESILIENT DESIGN OF STEEL FRAME BUILDINGS

Amedebrhan ASFAW[1], Fei SHI[2] & Osman OZBULUT[3]

Abstract. *This study discusses the development and experimental characterization of a new seismic damper that can provide stable energy dissipation with high self-centering capabilities. The proposed system, called as superelastic friction damper (SFD), leverages advantages offered by superelastic shape memory alloy (SMA) cables to create a full-scale seismic damper that integrates multiple functionalities such as repeatable energy dissipation, optimal self-centering capacity, high deformability, and reusability in a compact, easily scalable, and affordable system. SMA cables can provide large axial forces and exhibit superior mechanical properties compared to similar sized monolithic SMA bars at a substantially lower cost. As a result of their inherent superelastic material behaviour, when used in the proposed seismic protection system, SMA cables enable self-centering ability without the need for pre-tensioning, offer reliable performance at large deformation levels, and allow the reuse of the system after repetitive loading cycles. In this work, a description of the fundamental working principle of the SFDs is presented. The fabrication process and extensive experimental testing on a prototype damper is described. The effects of loading rate on the damper characteristics are evaluated. Then, a numerical model that can accurately capture response of the SFDs is developed. An eight-story steel frame building is designed with both SFDs and conventional friction dampers. The seismic performances of the designed structural systems are evaluated and compared through nonlinear response history analyses.*

Introduction

Conventional buildings are at significant risk for extensive post-earthquake downtime. In urban areas, this can lead to a significant economic recession. A highly influential factor in post-earthquake building downtime is a structure's ability to re-center after a large seismic event. One of the promising strategies for design of self-centering structural systems is the using shape memory alloy (SMA)-based seismic protection systems. The family of SMA-based dampers and energy dissipators for structural control continues to grow due to increasing interest in self-centering structural systems. Numerous prototypes of SMA dampers have been proposed, numerically studied, experimentally tested, and currently at various development stages (Ozbulut et al., 2011).

SMAs can be produced in different forms such as wires, cables, bars, or springs. However, most of existing SMA-based seismic devices available in the literature have employed the SMA wires as they are more widely available. This led to development of devices with low force capacity. Other forms of SMA such as helical springs, Bellville ishers, and plates have been shown promising results to increase the capacity of dampers or braces (Wang et al., 2019; Wang et al., 2020). However, these products are not readily available in the market and usually their cost is considerably higher. Moreover, the fabrication process of devices equipped with helical springs or Bellville ishers is more complicated and sensitive on construction precisions.

SMA cables have recently been suggested as a more convenient form of SMAs that can accommodate high force demands of structural applications (Ozbulut et al., 2016; Shi et al., 2022). An SMA cable is composed of multiple strands. Each strand has a core wire around which other SMA wires are twined. Given the advantages offered by the SMA cables, there is a growing interest in using SMA cables for seismic applications, specifically in bracing systems and dampers (Shi et al., 2020; Cao et al., 2022).

[1] Graduate student, University of Virginia, Charlottesville, VA, USA, amedebrhan.asfaw@vdot.virginia.gov
[2] Post-doctoral research associate, Guangzhou University, Guangzhou, China, shifei@gzhu.edu.cn
[3] Associate Professor, University of Virginia, Charlottesville, VA, USA, ozbulut@virginia.edu

Another challenge for SMA-based seismic control systems is the limited damping capacity of SMAs. The inherent energy dissipation capacity of SMAs is usually inadequate to render. When SMA-only dampers are used in a building, it can effectively control peak and residual displacement response. However, they could lead to an increase in floor acceleration response, consequently, damage to acceleration sensitive non-structural components. Note that damage to non- structural components often accounts for the majority of economic losses in an earthquake (Potter et al., 2015). In addition, a detrimental high-mode effect could be induced due to limited damping (Qui and Zhou, 2016).

In this study, a new SMA-based damper called, Superelastic Friction Damper (SFD), is proposed. The proposed damper leverages the high tensile resistance and superior self-centerig capability of SMA cables and the prominent damping capacity of a friction device. In what follows, a detailed description of experimental and numerical investigations on this device is presented.

Superelastic friction damper

Figure 1 shows an exploded view of the SFD. The damper comprises SMA cables, inner and outer steel members, friction pads, slotted end plates, and connection plates. The outer member consists of a pair of steel channels with bonded friction pads on the outside face of the web. The inner member is made up of I-shaped steel, in which the web serves as a sliding interface for the friction pads. The selection of appropriate friction interface material is vital to achieve long-term stable sliding behavior. In this study, friction pads made out of metal-free brake and clutch lining (also termed non-metallic melded strip) are used. The use of a brake lining pad against stainless steel (BL-SS) makes the sliding interface self-lubricate. As a result, the stick-slip phenomenon decreases, and a constant coefficient of friction is obtained independent of the loading rate. Furthermore, the sliding interface is resistant to rust and can provide long-term stable behaviour.

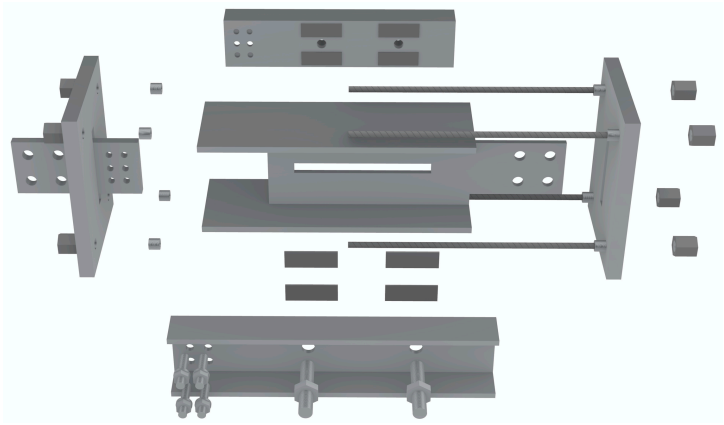

Figure 1. Exploded view of superelastic friction damper (SFD)

Experimental investigations

Test description

A proof-of-concept damper is designed and fabricated. The geometric details of the specimen are given in Figure 2. The sizes of the main parts are determined according to the following basic rules: (1) the strengths of the inner member, outer member, and other accessories are significantly larger than the maximum possible load resistance of the SMA cables plus the frictional force; (2) the length of the outer and inner members, as well as the distance between the end plates, is dictated by the length of SMA cables, which is determined by the stroke. Both members are made up of low carbon steel (nominal yield strength of 248 MPa).

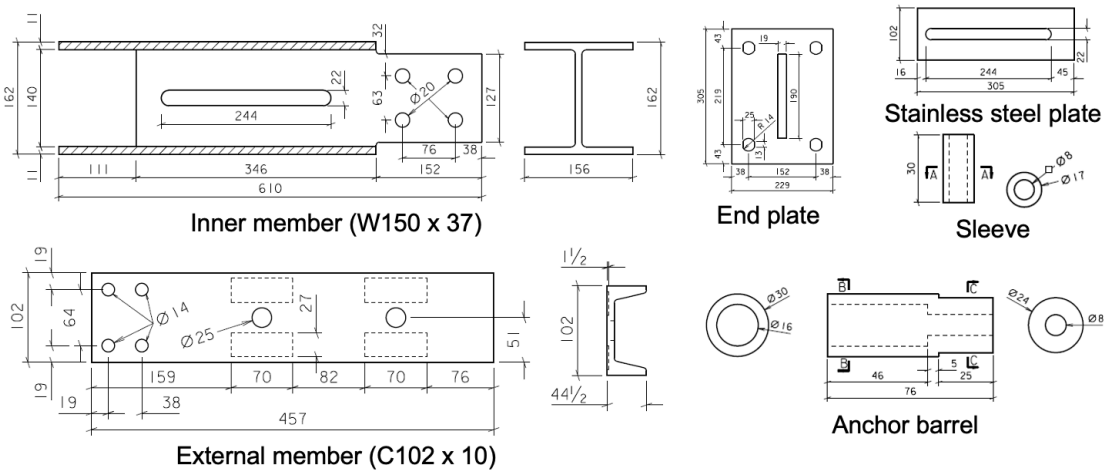

Figure 2. Damper specimen geometric details (unit: mm).

The cyclic loading tests are conducted to characterize hysteretic behavior of SFD. The SFD specimen is connected to an MTS 244 hydraulic actuator, which enables a maximum force of 98 kN and a maximum velocity of 381 mm/sec (Figure 3). The damper force and deformation are measured using built-in load cell and LVDT of the actuator. Two LCWD load isher and compression load cells are used to measure the compression force generated from two friction bolts. The response of the damper at frequencies ranging from 0.05 Hz to 1 Hz is characterized.

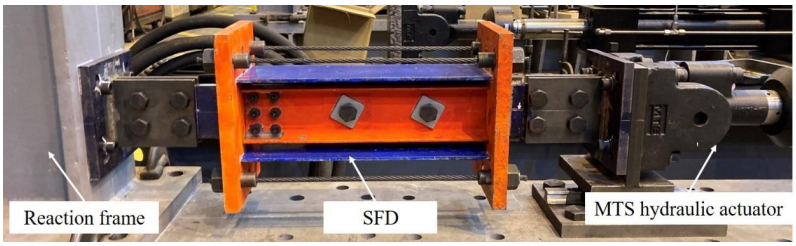

Figure 3. Experimental setup

Experimental results

Figure 4 shows the force-displacement response of the damper in the absence of the SMA cables, i.e., frictional component only. The response of the frictional component is shown under a quasi-static loading with a displacement amplitude incrementally increasing up to 30 mm. The hysteresis curves are plotted separately for four loading frequencies, namely, 0.05, 0.1, 0.5, and 1 Hz, at a constant amplitude of 25 mm. In general, the damper displayed a completely stable, repeatable, and reliable behaviour with insignificant dependence on the frequency for the range considered in this study.

Figure 5 shows the force-displacement response of the SFD under different loading frequencies. The overall response of the damper is consistent with the intended working principle. The behaviour of the damper in the two loading directions look symmetrical. As can be seen from Figure 5, there is also no significant effect of loading frequency on the damper response.

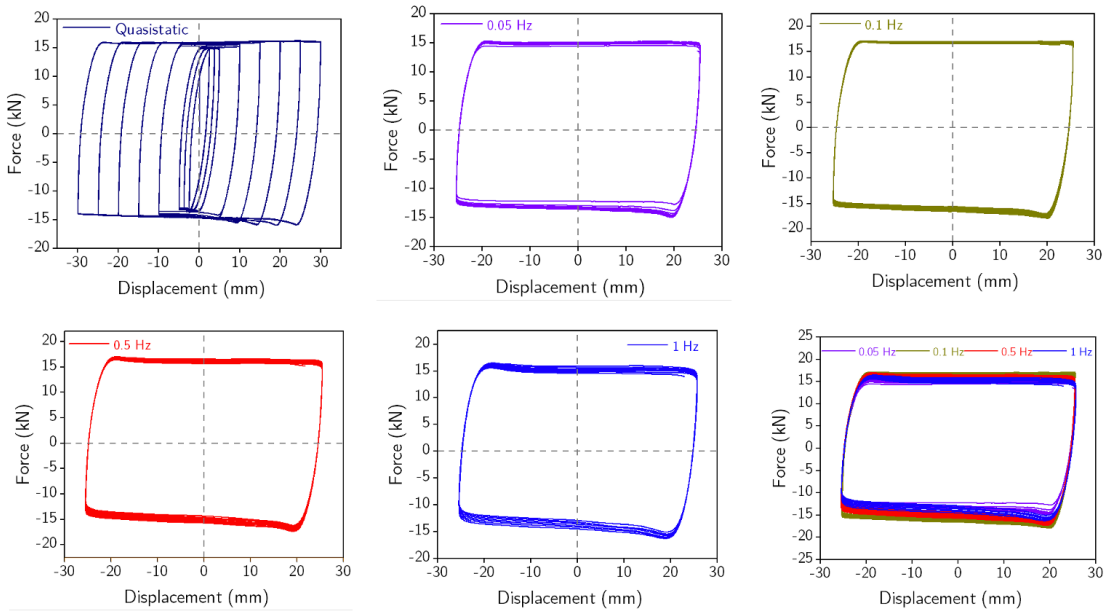

Figure 4. Force-displacement hysteresis curves of friction only damper under different loading frequencies

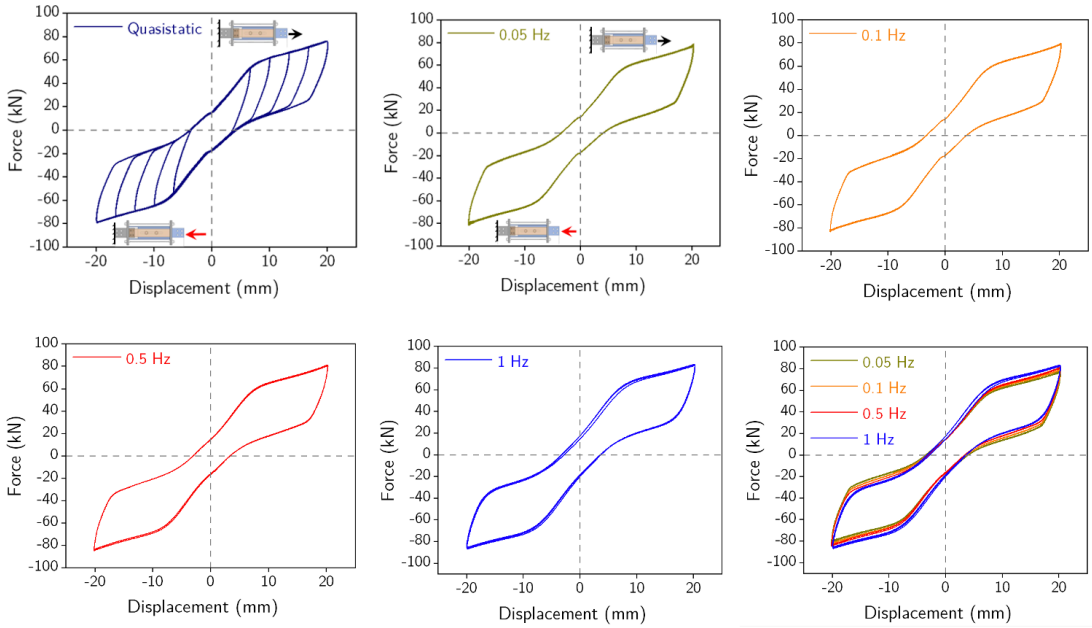

Figure 5. Force-displacement hysteresis responses of SFD under different loading frequencies

Numerical investigations

Description and modeling of prototype building

A four-story archetype steel-framed office building described in a NIST report (Speicher et al., 2020) is adopted in this study. Building's lateral load resisting capacity is provided by special steel moment resisting frame (SMRF) along the East-West (E-W) direction and special steel concentrically braced frame (SCBF) along the North-South (N-S) direction. All lateral force-resisting systems are symmetrically located at the perimeter of the building and orthogonal. The building is rectangular in plan, with five 9.14 m (30 ft) bays in the E-W direction and five 6.14 m (20 ft) bays in the N-S direction. The typical floor framing plan and elevation view are shown in Figure 6. All the analyses are based on one of the perimeters SMRF that serve as the lateral force resisting system of the building in the E-W direction. The building is located where it is assumed it would be assigned a Seismic Design Category (SDC) D_{max}. The fundamental period of the building is 2.2 seconds.

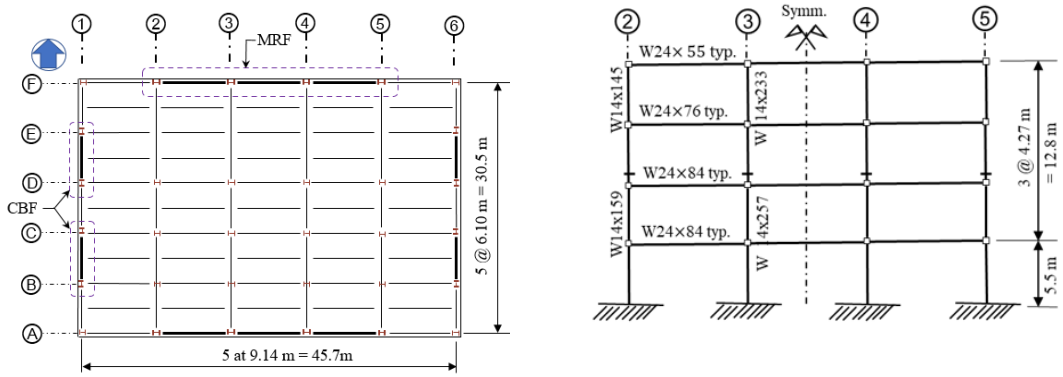

(a) *(b)*

Figure 6. Four-story steel frame building: (a) Floor plan and (b) elevation

A two-dimensional nonlinear model of the SMRF with panel zone (PZ) and reduced beam section (RBS) is created in the OpenSees structural analysis package. The plane frame elements of the structure are modelled as elastic beam-column elements with concentrated inelastic rotational springs. A bilinear hysteretic material model based on the modified Ibarra Medina Krawinkler (IMK) deterioration model is used for the plastic hinges to capture cyclic and in-cycle strength and stiffness degradations. The RBS connection stiffness is modelled using a prismatic cross-section over the length of the RBS. The width of the RBS is assumed to be equivalent to the actual RBS width at center. The PZ is simulated as a rectangle composed of a set of "rigid" elements connected by simple pin connections at the three corners and a zero-length rotational spring placed at the other corner to simulate the shear distortions in the PZ. A leaning column is employed to capture the *P-delta* effects arising from the forces acting on the deformed geometry.

The provisions of ASCE 7-16 Chapter 18 that deals with design of structures with added damping devices is adopted for the design. Thus, a reduced strength version of the fully code-compliant frame is developed first by selecting smaller beam and column member sizes such that the frame has a base shear capacity equal to 75% of the base shear capacity of the original SMRF. The reduced strength frame satisfies the strength requirements of the design codes but violates the drift limits. The SFDs are then designed with the objective of complying with the story drift requirements and to provide similar stiffness with the original SMRF. The SFDs are installed at each bay of each story level using a chevron configuration. The selected member sizes for the beams and columns as well as a typical installation scheme of the SFD are shown in Figure 7(a).

The SFDs are modelled using parallel combinations of self-centering springs and a spring assigned with steel02 material. Figure 7(b) compares the experimental results of the quasi-static loading test at room temperature with model prediction. The numerical model can successfully reproduce the experimental response of the SFD. In a typical damper, the area of SMA cables is calculated to be 482 mm^2 and the friction force is 52 kN to satisfy the design objectives mentioned above. The selected SFD design parameters can be considered as four times larger than the prototype damper tested. The dampers in all floors are assumed the same.

To check validity of the designed frame fulfilling the code drift requirements, nonlinear response history analyses are performed. A total of 7 ground motions are selected from the PEER NGA strong ground motions database and scaled in accordance with the ASE 7-16. The mean story drifts for design level earthquakes for the steel frame building is found to be 2.13%, while it was 2.16% for the steel building with SFDs, both of which are lower than allowable story drift of 2.5%.

To obtain an overall understanding on the global behaviours of the uncontrolled and controlled frames, a displacement-driven monotonic pushover analysis is conducted. In this way, it allows a quantitative comparison of the lateral strength and post-yield behaviour of each frame under progressive loading process. Figure 8 shows the results of the pushover analyses when the frames are subjected to a static lateral force with first-mode pattern based on ASCE 7-16.

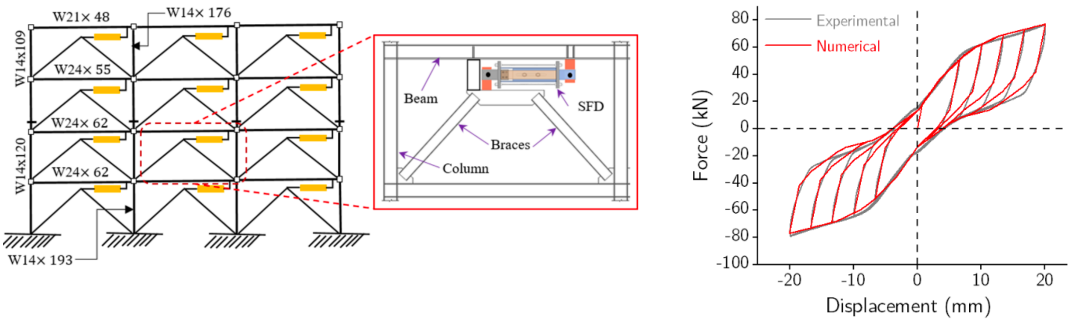

(a) (b)

Figure 7. (a) A four-story steel moment resisting frame installed with SFDs; (b) comparison between experimental result and proposed model prediction.

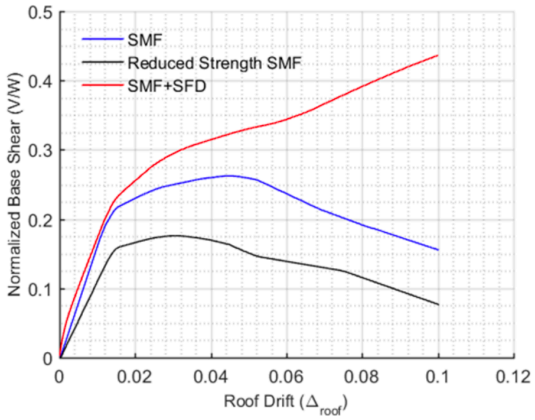

Figure 8. Pushover curves of original steel frame, reduced strength frame, and steel frame with SFD

Ground Motion Selection

A total of 14 strong motion records are used in the nonlinear response history analyses. The records are selected from the FEMA P-695 far-field record set and are normalized for magnitude, distance, and source conditions as discussed in the report. The ground motion scaling procedure follows the ASCE 7-16 guidance. Figure 9 illustrates the set of acceleration response spectra, original and scaled, and the scaled average spectrum. Target spectra for the MCE level developed using the site spectral acceleration values provided in ASCE 7-16 and described in previous section is also shown in the figure. The mean spectrum of the 14 records is not less than the target response spectrum for period ranging from $0.2\times T_1$ to $1.5\times T_1$, where T_1 is the fundamental period of vibration for the frame. Therefore, code requirements are satisfied.

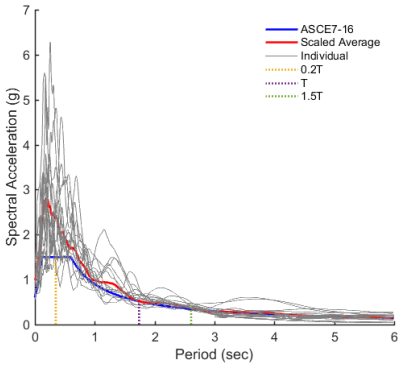

Figure 9. Acceleration response spectra for scaled ground motions and average spectrum

Seismic performance assessment

The seismic responses of the steel frame with and without SFDs are evaluated by subjecting them to realistic earthquake ground motion records. The 14 ground motions are used to provide a basic performance assessment under two different seismic hazard levels: Design Basis Earthquake (DBE) and Maximum Considered Earthquake (MCE). The acceleration time history of each ground motion record is followed by zero values for 10 seconds, with the aim to allow structural vibration to decay and to accurately record the residual deformation. The selected engineering demand parameters for the performance evaluation include: peak interstory drift ratio (PID), residual interstory drift ratio (RID), and peak floor acceleration (PFA). The PID is selected as an important performance index since it can be correlated with damage in structural elements, while the PFA indicates damage to acceleration sensitive non-structural components. The post-earthquake functionality of buildings is determined based on the RID.

Figures 10 and 11 show the PID, RID, and PFA for the uncontrolled and controlled frames for each ground motions scaled to DBE and MCE levels, respectively. It is evident that the SFDs significantly reduces the drift demand of the controlled frame under both levels. The structure experienced negligible residual drift. A set of RID limits are stipulated in FEMA P-58 (2018). Several damage state classes are described as: DS1, which restricts the RID to less than 0.2%, such that “no structural realignment is necessary for structural stability, but the building may require adjustment and repairs to non-structural and mechanical components. A more relaxed second class, DS2, requires RID to be less than 0.5%, such that realignment of structural frame and related structural repairs are economically feasible, and degradation in structural stability is limited. In light of these restrictions, the analysis results show that the controlled frame easily meets class DS1 in almost all earthquake records due to the excellent self-centering capability of the SFDs. On the contrary, the uncontrolled frame exceeds the 0.5% threshold in nine earthquake records. Therefore, expensive repair works are inevitable for the latter case.

The PFA response of the controlled frame increased slightly compared with the uncontrolled frame. The absolute floor acceleration response is directly associated with the difference in interstory shear forces of two adjacent floors. Compared with SMRF, the flag-shaped hysteretic behaviour of the SFD has more frequent transitions along the unloading path, and as a result an instantaneous high amplitude PFA pulse is more likely to be produced during an earthquake loading. Nevertheless, the amplification is less than 10% on average, and if needed, it can be effectively controlled by adjusting the SFD design parameters.

Figure 12 shows the mean height-wise profiles of the PID, RID, and PFA of the uncontrolled and controlled frames under the DBE and MCE seismic hazard levels. It can be seen that the PID mostly uniformly distributed along the height of the controlled frame and it is effectively reduced in all stories. Specifically, the mean PID reduced from 2.2% to 1.3% at DBE and from 3.57% to 1.90% at MCE, corresponding to 41% and 47% reductions, respectively. The results clearly demonstrate the efficacy of the SFDs in effectively reducing the displacement demand of the steel frame. Uniform distribution of drifts in structures is of paramount importance which is not generally satisfied in compliance with the state-of-the-art seismic provisions. As such, to avoid drift concentrations and soft-story failures, optimum distribution of stiffness and strength should be acquired, which can be realized by installing supplemental damping devices such as the SFD.

Regarding the RID responses, the mean response of the uncontrolled frame violates the DS1 and DS2 requirements at both hazard levels, whereas, the controlled frame meets DS1 requirement with sufficient safety margin at DBE and just meet the limit at MCE. The mean maximum residual interstory drift ratio among all the floors under DBE and MCE levels are dramatically decreased by 95% and 90%, respectively, after the dampers are installed. It is also observed that the PFA slightly amplified in the upper floors.

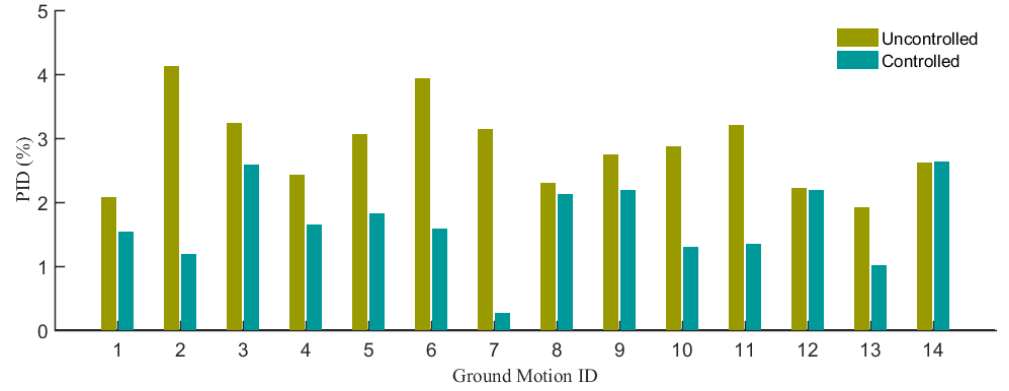

(a)

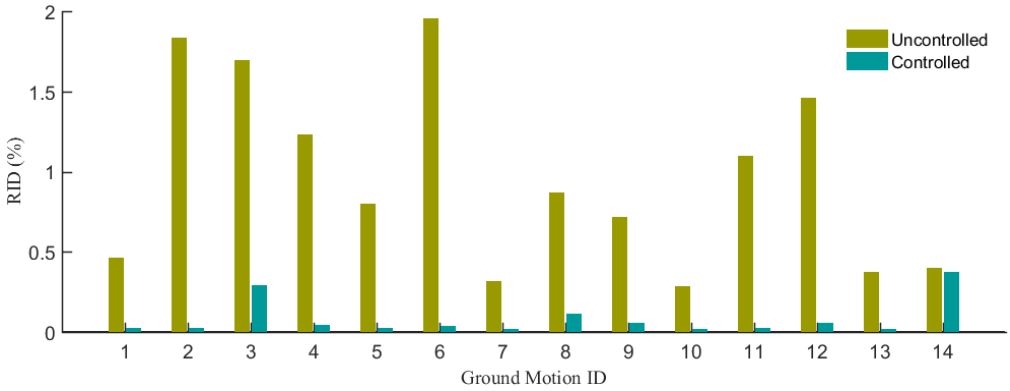

(b)

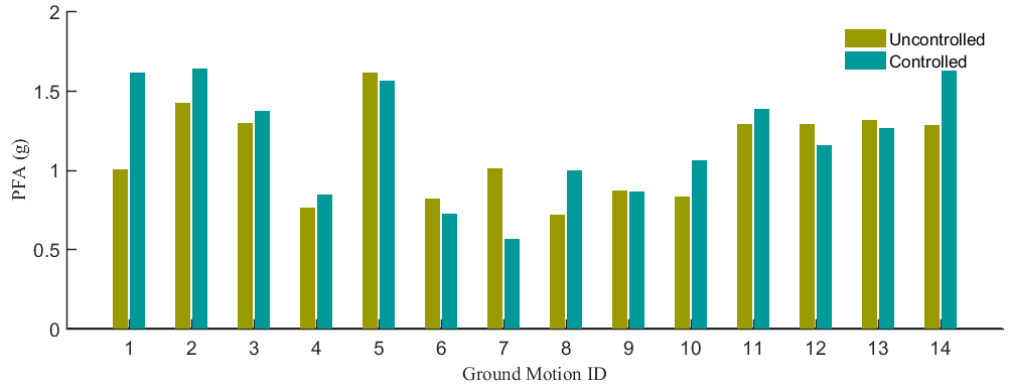

(c)

Figure 10. Engineering demand parameters: (a) IDR, (b) RDR, and (c) PFA of controlled and uncontrolled frames subjected to ground motions scaled to DBE level

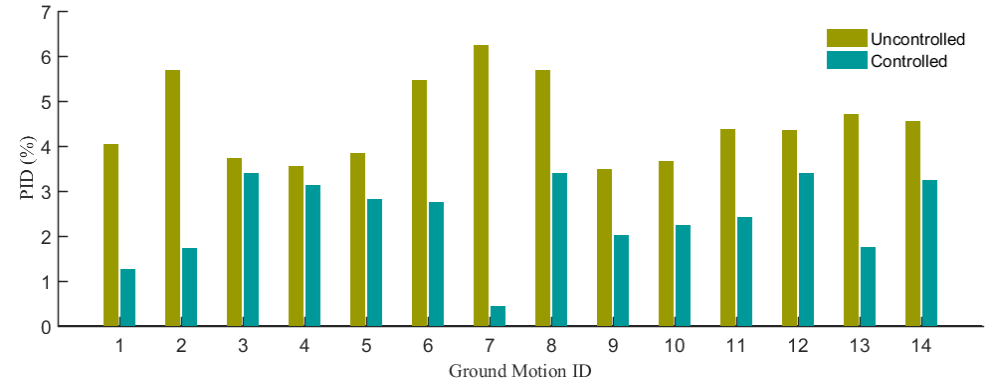

(a)

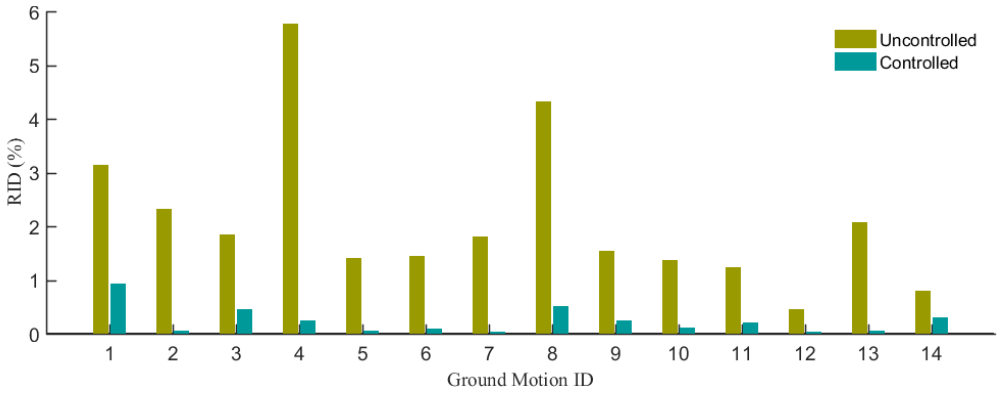

(b)

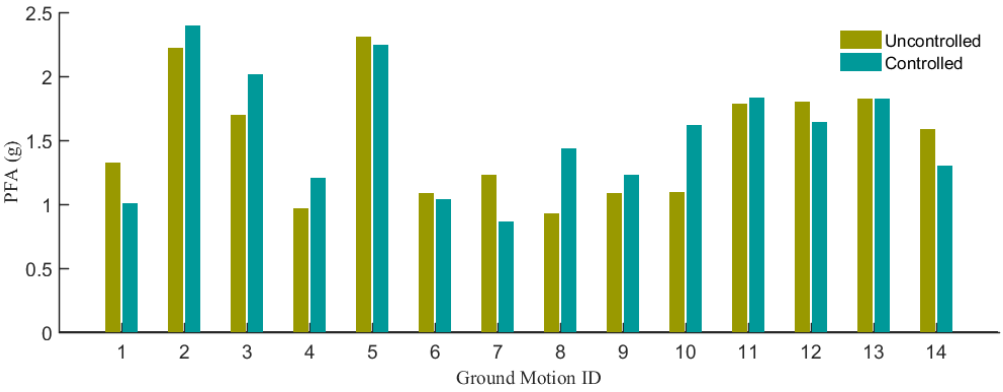

(c)

Figure 11. Engineering demand parameters: (a) IDR, (b) RDR, and (c) PFA of controlled and uncontrolled frames subjected to ground motions scaled to MCE level

Conclusions

In this paper, the working mechanics and fabrication process of a prototype damper are first introduced, followed by a detailed experimental investigation on a large-scale prototype damper. Moreover, nonlinear response history analyses of a four-story special steel moment-resisting frame installed with the SFD are conducted to evaluate the efficacy of the damper in controlling the response of the frame. Throughout the entire experimental program, the proposed damper exhibited a completely stable, repeatable, predictable, and reliable flag-shaped behaviour without strength and stiffness degradation and negligible dependence on the loading frequency. No damage is observed to any of the damper components, highlighting that a damper installed in a structure and subjected to an earthquake loading would perform well during subsequent earthquakes without the need for the replacement or substantial repair. Based on the results obtained from numerical simulations, it can be concluded that the SFD can significantly reduce

or essentially eliminate residual drifts while providing almost the same performance to acceleration-sensitive non-structural components as conventional SMRF.

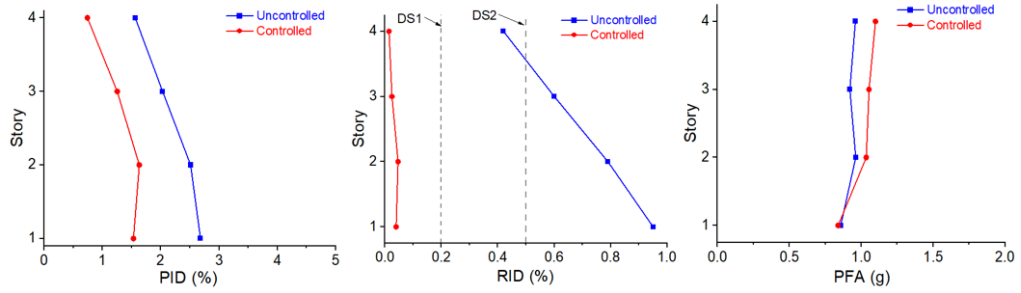

(a)

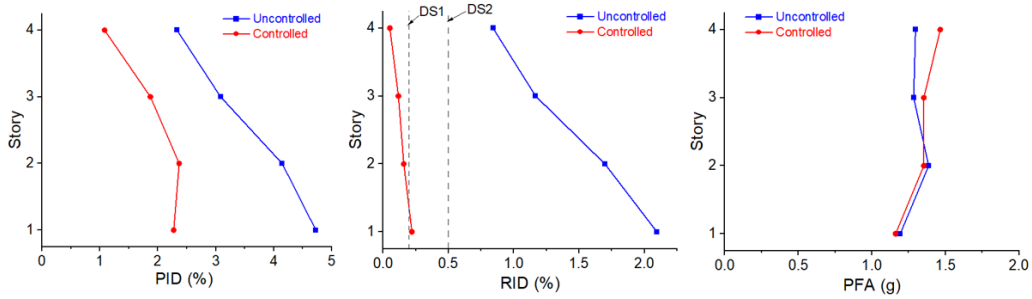

(b)

Figure 12. Comparisons of engineering demand parameters (IDR, RDR, and PFA) between uncontrolled and controlled frames at: (a) DBE and (b) MCE levels

References

Cao S, Ozbulut OE, Shi F and Deng J (2022), An SMA cable-based negative stiffness seismic isolator: Development, experimental characterization, and numerical modelling, *Journal of Intelligent Material Systems and Structures*, 33(14), 1819-1833.

FEMA (2018), Seismic performance assessment of buildings, volume 5 - expected seismic performance of code-conforming buildings, FEMA P-58-5 5 196.

Ozbulut OE, Hurlebaus S and DesRoches R (2011). Seismic response control using shape memory alloys: a review, *Journal of Intelligent Material Systems and Structures*, 22(14), pp.1531-1549.

Ozbulut OE, Daghash S and Sherif MM (2016). Shape memory alloy cables for structural applications, *Journal of Materials in Civil Engineering*, 28(4), p.04015176.

Qiu CX and Zhu S (2016), High-mode effects on seismic performance of multi- story self-centering braced steel frames, *J. Constr. Steel Res*, 119 133–43.

Potter SH, Becker JS, Johnston DM and Rossiter KP (2015). An overview of the impacts of the 2010-2011 Canterbury earthquakes, *Int. J. Disaster Risk Reduct*, 14 6–14.

Shi F, Ozbulut, OE, Li Z, Wu Z, Ren F and Zhou Y (2022), Effects of ambient temperature on cyclic response and functional fatigue of shape memory alloy cables, *Journal of Building Engineering*, 52, 104340.

Shi F, Ozbulut OE and Zhou Y (2020), Influence of shape memory alloy brace design parameters on seismic performance of self-centering steel frame buildings, *Structural Control and Health Monitoring*, 27(1), p.e2462.

Speicher MS, Dukes J and Wong KKF (2020). Collapse risk of steel special moment frames per FEMA P695. NIST Technical Note 2084 97.

Wang B, Zhu S, Chen K and Huang J (2020), Development of superelastic SMA angles as seismic-resistant self-centering devices, *Engineering Structures*, 218 110836

Wang W, Fang C, Zhang A and Liu X (2019), Manufacturing and performance of a novel self-centring damper with shape memory alloy ring springs for seismic resilience, *Struct. Control Heal. Monit.,* 26 1–17